Neurochemistry International 60 (2012) 640–651

Contents lists available at SciVerse ScienceDirect

Neurochemistry International

journal homepage: www.elsevier.com/locate/nci

AGEs–RAGE mediated up-regulation of connexin43 in activated human microglial CHME-5 cells

Shamim B. Shaikh *, Benedict Uy, Amali Perera, Louise F.B. Nicholson

Department of Anatomy with Radiology and The Centre for Brain Research, Faculty of Medical and Health Sciences, University of Auckland, Private Bag 92019, Auckland, New Zealand

ARTICLE INFO

Article history:
Received 15 September 2011
Received in revised form 14 December 2011
Accepted 21 February 2012
Available online 6 March 2012

Keywords:
Human microglia
CHME-5
AGEs
RAGE
Connexin43
TNFRII

ABSTRACT

Microglial activation is a significant contributor to the pathogenesis of many neurodegenerative diseases. Microglia respond to a range of stimuli including pathogenic protein deposits such as advanced glycation endproducts (AGEs). AGEs are prominent inflammatory stimuli that accumulate in the ageing brain. AGEs can activate microglia, leading to the production of excessive amounts of inflammatory cytokines and coupling via gap junction proteins especially connexin43 (Cx43). The literature on the expression of microglial Cx43 during inflammation is controversial. Many cellular effects of AGEs are thought to be mediated by the receptor RAGE. There is however, no evidence suggesting Cx43 is a downstream effector of AGEs–RAGE interaction in microglia. In addition, most of the AGEs-related studies have been undertaken using rodent microglia; the information on human microglia is sparse. Microglia of human and rodent origin respond differently to certain stimuli. The aims of this study were to investigate the AGEs–RAGE-mediated activation of human microglia and establish if Cx43 is one of the downstream effectors of AGEs–RAGE interaction in these cells. Human microglial CHME-5 cells were treated with different doses of AGEs for a selected time-period and microglial activation studied using specific markers. The protein expression of RAGE, Cx43 and TNF-α-receptors (RI and RII) was analysed in response to AGEs in the absence/presence of various doses of anti-RAGE Fabs. TNF-α levels in media were measured using ELISA. TNF-α-induced opening of gap junctional channels was assessed by dye uptake assays and the effect of neutralising TNFRII on Cx43 levels was also studied. CHME-5 cells showed an up-regulation of RAGE, TNF-α, TNFRs (especially TNFRII) and Cx43 upon AGEs treatment and a significant dose-dependent drop in the levels of TNF-α, TNFRII and Cx43 in the presence of anti-RAGE Fabs. TNF-α induced gap junctional/hemichannel opening whereas blocking TNFRII inhibited TNF-α-induced increase in Cx43 levels. Results suggested that TNF-α, TNFRII and Cx43 are downstream effectors of the AGEs–RAGE interaction in human microglial CHME-5 cells.

1. Introduction

Microglia are the resident immune cells of the central nervous system (CNS) and are readily activated in response to infection or injury (McGeer and McGeer, 1997; Nagatsu and Sawada, 2007; Shavali et al., 2006). Activated microglia up-regulate a variety of surface receptors and secrete a host of soluble factors. While the early stages of microglial activation preserve homeostasis, prolonged (chronic) activation produces a cocktail of pro-inflammatory cytokines (such as TNF-α, IL-1β and IFN-γ) (Kawanokuchi et al., 2006; McGeer and McGeer, 1997; Nagatsu and Sawada, 2007; Shavali et al., 2006) with the benefits of the initial microglial activation being overshadowed by harmful effects of inflammatory cytokines. Evidence from post mortem studies of human brains (McGeer and McGeer, 1997; McGeer et al., 1988), *in vitro* (Munch et al., 2003; Takeuchi et al., 2006) and *in vivo* (Sherer et al., 2003) studies has established an association of chronic microglial activation with neurodegeneration in several diseases (Lawson et al., 1990; McGeer et al., 1988).

Microglia may be activated directly, by foreign substances such as lipopolysaccharides (LPS) found on bacterial cell walls (Gao et al., 2002), toxins such as trimethyline (Eskes et al., 2003), unregulated increases in normal endogenous substances such as cytokines, factors released by mechanically injured neurons (Eskes et al., 2003), increased levels of reactive oxygen species (ROS), and by the chronic accumulation of pathogenic protein molecules such as

Abbreviations: AGEs, advanced glycation endproducts; Cbx, Carbenoxolone; Cx43, connexin43; Fab, fragment antigen-binding; Fc, fragment crystallizable region; GAPDH, Glyceraldehyde 3-phosphate dehydrogenase; GJC, gap junction channels; $LaCl_3$, Lanthanam (III) chloride; RAGE, receptor for advanced glycation endproducts; TNF-α, tumour necrosis factor-alpha; TNFRI, tumour necrosis factor-α receptor I; TNFRII, tumour necrosis factor-α receptor II.

* Corresponding author. Tel.: +64 9 8202214; fax: +64 9 373 7484.
E-mail addresses: shamims@xtra.co.nz, s.shaikh@auckland.ac.nz (S.B. Shaikh), b.uy@auckland.ac.nz (B. Uy), amali_101@hotmail.com (A. Perera), lfb.nicholson@auckland.ac.nz (L.F.B. Nicholson).

0197-0186/$ - see front matter © 2012 Elsevier Ltd. All rights reserved.
doi:10.1016/j.neuint.2012.02.023

amyloid beta (Aβ) and advanced glycation endproducts (AGEs) (Dukic-Stefanovic et al., 2003). AGEs are a heterogeneous population of highly reactive compounds derived from non-enzymatic, multistep reactions between sugars and protein amino acid side chains and complex re-arrangements of glycated peptides (Schmitt et al., 2005a). Under normal physiological conditions, AGEs are formed at a very slow rate and accumulate with age in several tissues including the brain. The rate of accumulation of AGEs in various tissues/organs is accelerated under oxidative stress, and in inflammatory and hyperglycaemic conditions (Ramasamy et al., 2005). In addition to their endogenous production, AGEs are also introduced into the body through exogenous sources such as processed foods (Peppa et al., 2003). Accumulation of AGEs in human brains has been observed in Alzheimer's and Parkinson's disease (Dalfo and Ferrer, 2005; Lue et al., 2005; Munch et al., 2000) where AGEs can exert their harmful effects on cells, particularly neurons, in several ways. AGEs can form protease resistant cross-links of long lived proteins that accumulate over time, as seen in the plaques in Alzheimer's disease (Lue et al., 2005) or intra-neuronal inclusion bodies (Lewy bodies) seen in Parkinson's disease (Munch et al., 2000). AGEs can also affect neurons via the activation of microglia. AGEs-mediated activation of rodent microglia, monocytes and macrophages results in activation of the NF-kB pathway and increased production of cytokines including TNF-α and IL-6 (Munch et al., 2003; Neumann et al., 1999; Wang et al., 2007). These cytokines increase cellular communication via gap junctions comprised of proteins knows as connexins (Cx) especially Cx43 in primary rodent microglia (Eugenin et al., 2001), and induce microglial glutamate release via Cx hemichannels (Takeuchi et al., 2006). Glial Cxs are known to contribute to neuroinflammation and neurodegeneration (Kielian, 2008).

Most of AGEs-mediated effects are believed to be via binding of AGEs to cell surface receptors (Schmitt et al., 2006). There are several receptors for AGEs and some of them contribute to AGEs-mediated effects observed. However, the well-characterised, multi-ligand signal transduction receptor RAGE (Receptor for AGEs) is a major player in mediating the cellular effects of AGEs (Lue et al., 2005; Schmitt et al., 2006). AGEs–RAGE interaction has been implicated in several chronic late onset diseases including Alzheimer's and Parkinson's disease (Dalfo et al., 2005; Lue et al., 2005). The effects of AGEs have been documented primarily in microglia, monocytes and macrophages of rodent origin; the information on human microglia is sparse. To the best of our knowledge, only one study has shown AGEs-mediated ROS generation in CHME-5 human microglial cell line (Schmitt et al., 2006) with one other study using human primary microglia to investigate Aβ–RAGE interaction (Lue et al., 2001). The biology of AGEs and RAGE is complex; each of these molecules can react with multiple proteins (receptors or ligands respectively) and activate various signalling pathways depending on the proteins to which they bind (Ramasamy et al., 2005; Schmidt et al., 2000; Schmitt et al., 2006) leading to cell type specific responses. Differences in response to the same stimulus have also been observed between microglia of human and rodent origin (Colton et al., 1996; Dragunow, 2008; Schmitt et al., 2006). The aims of the present study were therefore to investigate the effects of exogenous AGEs on human microglial CHME-5 cells and the downstream effectors involved in the AGEs–RAGE interaction in these cells.

2. Material and methods

2.1. Cell culture

CHME-5 cells (a generous gift from Professor Pierre Talbot, Laboratory of Neuroimmunovirology, INRS-Institute, Armand-Frappier, Canada) were used in this study. These cells were derived from human foetal microglia through transformation with SV-40 virus (Atanassov et al., 1995; Peudenier et al., 1991). CHME-5 cells express the antigens present on adult human microglia, secrete pro-inflammatory cytokines upon activation and exhibit several properties of primary human microglia. CHME-5 cells have been used successfully by us (Shaikh and Nicholson, 2009) and others (Atanassov et al., 1995; de Gannes et al., 1998; Macouillard-Poulletier de Gannes et al., 2000) in previous studies. Most of the experiments in this study were carried out using cells from early passages (P11–P15 passages). For routine cultures, cells were grown as described previously (Shaikh and Nicholson, 2009). Briefly, cells (1.7×10^2 cells/25 cm^2) were grown in complete DMEM-F12 (Dulbecco's Modified Eagle Medium-F12) medium with 10% FBS (Foetal Bovine Serum), 2 mM glutamine and 1 mM sodium pyruvate at 37 °C under 5% CO_2 in humidified air. Antibiotics were not used at any step.

2.2. Preparation of AGEs

The method of AGEs preparation in our laboratory has been described previously (Shaikh and Nicholson, 2006, 2008). The method has been modified slightly for this study. AGEs were prepared by incubating 0.1 mM BSA (Fraction V, culture grade, Invitrogen Inc, USA) with 1 M glucose in sterile PBS, pH 7.4 at 50 °C for 6 weeks. All solutions used were filter sterilized and all incubations carried out in sterile conditions. After incubation the samples were dialysed for 48 h to remove unbound sugars; the dialysis process was repeated three times using PBS buffer. Dialysed AGEs were filter sterilized and stored at −80 °C until required. The AGEs preparation was analysed for the presence of bacterial endotoxins using a quantitative, E-toxate endotoxin assay kit (Sigma Aldrich, USA) according to the manufacturer's instructions (endotoxins could not be detected in the AGEs preparation). Protein concentrations were estimated by the Bradford protein assay (Bio-Rad, USA) using BSA standards. AGEs contents were determined by taking optical measurements (OD at 405 nm; 0.588/mg protein) as previously described (Kuhla et al., 2004; Munch et al., 2000) and carbonyl content determined by performing the biochemical 2, 4-dinitrophenylhydrazine (DNP) assay (data not shown). This assay is used to monitor the extent of protein modification and assesses the irreversible modification of proteins during glycation (Schmitt et al., 2005b; Valencia et al., 2004); the assay is described briefly at the end of this paragraph. The presence of AGEs was also confirmed by running the samples on a 10% SDS–Polyacrylamide (SDS–PAGE) gel and performing western blot using the monoclonal anti-AGE 6D12 antibody (TransGenic Inc, Japan). The CML epitope of AGEs serves as the ligand for RAGE (Schmidt et al., 2000; Yan et al., 2003). The presence of the CML complexed BSA/proteins was detected using an anti-CML antibody (KAL-KH024, TransGenic Inc, Japan) (data not shown). The concentration of AGEs-modified proteins was calculated using the molecular weight of the non-glycated BSA. For control, 0.1 mM BSA in PBS was processed in similar conditions.

2.2.1. 2, 4-Dinitrophenylhydrazine (DNP) assay

This method was modified from Valencia et al., (Valencia et al., 2004). For the DNP assay, the AGEs samples (0.2 ml) were mixed with 0.5 ml of 4 mg/ml BSA (carrier protein) in PBS followed by the addition of an equal volume of 0.1% DNP (in 2 M HCl). The mixture was incubated at room temperature for 1 h, followed by precipitation with 30% TCA (Trichloro acetic acid) on ice for 30 min. The precipitate was centrifuged (14,000 $g \times 5$ min) and the pellet washed three times in 1:1 ethanol + ethylacetate solution. The pellet was dissolved in a guanidine hydrochloride solution (0.3 ml of 8 M guanidine hydrochloride, 13 mM EDTA, and 133 mM Tris at

pH 7.4), centrifuged and UV absorbance measured in the supernatant at 365 nm using the NanoDrop® ND-1000 spectrophotometer (V3.0.1, Analytical Technologies). Guanidine hydrochloride served as a blank and fresh BSA as a control. Results were expressed as mol of DNP per mol of protein sample.

2.3. Preparation of anti-RAGE and mouse IgG Fab fragments

To make anti-RAGE Fab (fragment antigen-binding) fragments, a Fab preparation kit from Pierce Biotechnology (Thermo Scientific, USA) and 200 μg of anti-RAGE monoclonal IgG (Chemicon, USA) were used. This kit contains the necessary components for simple generation of Fab fragments from antibodies. Preparation of Fab fragments is based on the principle of digestion of IgGs (antibodies) by the enzyme papain that cleaves IgGs into Fab fragments (retains the antigen-binding site) and Fc (fragment crystallizable region) fragments. The papain digestion is followed by the purification of the digest by removing undigested IgGs and Fc fragments using immobilized protein A columns. For a control, non-immune mouse IgGs were processed similarly to obtain mouse (Ms) Fabs. The final Fab solutions were quantified by UV absorption at 280 nm using a NanoDrop® ND-1000 spectrophotometer (V3.0.1, Analytical technologies) and purity of the samples checked by SDS–PAGE electrophoresis (Molecular weight of Fab fragments is 50 kDa).

2.4. Detection of microglial activation

Microglia are known to be activated in the presence of AGEs (Munch et al., 2003). To confirm that AGEs made in our laboratory activate CHME-5 cells, cells were grown using the culture media and conditions described above (Section 2.1) in the presence of different doses of AGEs (2, 5 and 10 μM for western blots and 5 and 10 μM for immunostaining) or 10 μM BSA. Cells were cultured in a 6-well plate to collect cell lysates for western blotting or in a 24-well plate on cover slips (13 mm diameter, positively charged, Superior Marienfeld, Germany) to collect cells for immunocytochemistry. Cell numbers were adjusted to achieve 90% confluency in each set. At the end of the treatment, cells on coverslips were fixed in 4% buffered paraformaldehyde (PFA) and processed for fluorescent immunocytochemistry to detect microglial activation using two markers widely used by us (Shaikh and Nicholson, 2009) and others (Graeber et al., 1994; Horikoshi et al., 2003; Sasaki et al., 2004), Glucose transporter type 5 (Glut-5) and CR3/43 (anti-HLA-DR/DQ/DP). Glut-5 is a microglial specific protein (Horikoshi et al., 2003; Sasaki et al., 2004) that contributes to the kinetics of cerebral metabolism. The expression of Glut-5 is detected at all stages of microglial activation, however its expression increases with activation (He and Crews, 2008). The CR3/43 antibody detects genes of the class II major histocompatibility complex (MHC class II) also known as HLA-DR/DP/DQ; these genes have important roles in the immune system. These MHC class II genes are expressed specifically in activated microglia (Graeber et al., 1994; Rogers et al., 1988; Sasaki et al., 1997). For immunocytochemistry, the primary antibodies for both markers, rabbit anti-human Glut-5 (AB1041, Chemicon International Inc, USA, 1:200 diluted) and monoclonal anti-CR3/43 (ab7856, abcam, UK, 1:100 diluted) were diluted in the appropriate blocking solutions. This was followed by incubations with their respective secondary antibodies (anti-rabbit Alexa 568 and anti-mouse Alexa 488 respectively, 1:400 diluted, Molecular Probes, USA). Following secondary antibody washes with PBS-T (PBS with 0.1% Tween 20), cells were treated with Hoechst 33258 nuclear dye (Molecular Probes, Invitrogen, USA; 1:500 diluted in PBS) for 5 min, washed with PBS-T and coverslips mounted with Prolong gold mounting medium (Molecular Probes, USA). Images were collected using a Leica DMR fluorescence microscope.

The CR3/43 marker increases upon activation, therefore AGEs dose-dependent microglial activation was also confirmed by western blotting for the CR3/43 marker in cell lysates obtained from three treatment groups (2, 5 and 10 μM AGEs) and controls. Each sample of 20 μg was loaded in individual wells of a 4–12% gradient SDS–Polyacrylamide (PAGE) gel and run at 200 V using MOPS buffer (NuPAGE, Invitrogen). A nitrocellulose membrane and transfer buffer (with 20% methanol, Invitrogen) were used to transfer proteins (at 30 V for 1 h at 4 °C). Membranes were blocked with 5% non-fat milk made in PBS-T for 16–18 h at 4 °C. After blocking, membranes were washed in PBS-T at room temperature (RT) followed by incubation for 3 h at RT with the primary monoclonal antibody for CR3/43 (ab7856, abcam, UK, 1:100 diluted). The membranes were then washed with PBS-T, followed by incubation with the HRP-conjugated anti-mouse antibody (1:8000 diluted, Sigma Aldrich, USA); both antibodies were diluted in 1% milk in PBS-T. An ECL-plus chemiluminescent kit (GE Healthcare, UK) was used to generate signals which were captured using a Fujifilm luminescent image analyser (LAS 4000 Version 2.0). Membranes were then stripped using stripping buffer (625 mM Tris, 2% SDS, 0.7% β-mercaptoehanol) and re-probed with anti-GAPDH (Glyceraldehyde-3-phosphate dehydrogenase) antibody (G9545, Sigma Aldrich, USA, 1:1000). GAPDH was used as a loading control and the intensity of the target normalised against that of GAPDH in respective wells and values expressed in densitometric units.

2.5. Treatment of CHME-5 cells with AGEs in the absence/presence of anti-RAGE Fabs

CHME-5 cells were grown in complete DMEM-F12 with 10% FBS and conditions as described in Section 2.1. Cell numbers were adjusted to reach confluency in 48 h in a 25 cm^2 culture flask (CELLSTAR®, Greiner Bio-One, Germany). Cells were assigned to seven treatment groups as listed below.

a. untreated controls
b. cells treated with 10 μM AGEs only
c. cells pre-incubated with 10 μg mouse Fabs (Ms Fab) + 10 μM AGEs
d. cells pre-incubated with 5 μg of anti-RAGE Fabs + 10 μM AGEs
e. cells pre-incubated with 10 μg of anti-RAGE Fabs + 10 μM AGEs
f. cells treated with 10 μg of anti-RAGE Fabs only
g. cells treated with 10 μM BSA only

Treatments were carried out for 24 h. Since anti-RAGE Fabs were made from the monoclonal antibody, non-immune Ms Fabs were used as a control to assess the specificity of anti-RAGE Fabs. For Fabs treatments, both Ms and anti-RAGE Fabs were pre-incubated for 4 h prior to addition of AGEs. BSA was the major protein component in the AGEs prepared in our laboratory; unmodified BSA was therefore used as a control to confirm that the effects seen in CHME-5 cells were AGEs specific. Culture media and cell lysates were collected from all treatment groups and stored at −20 °C.

2.6. Measurement of TNF-α

Culture media collected from all treatment groups were processed for measuring the levels of TNF-α using an ELISA kit specific for human TNF-α (Catalogue number 555212, BD Biosciences, Pharmigen, US), as per the manufacturer's instructions. TNF-α levels were expressed in both pg/ml of culture media and pg/gm of total protein in cell lysates.

2.7. Detection of RAGE, connexin43 (Cx43), TNFRI and TNFRII

The levels of RAGE, Cx43, TNFRI and TNFRII (relative to the loading control) were estimated in cell lysates obtained from the seven treatment groups using western blot methods as described in Section 2.4 and specific antibodies. Primary antibodies used were mouse anti-RAGE (MAB5328, Chemicon, USA, 1:1000), rabbit anti-connexin43 (C6219, Sigma Aldrich, USA, 1:800), goat anti-TNFRI (AF225, R & D Systems Inc, USA, 1:1000), mouse anti-TNFRII (MAB226, R & D Systems Inc, USA, 1:500) and rabbit anti-GAPDH (G9545, Sigma Aldrich, USA, 1:1000). HRP-conjugated secondary antibodies (Sigma Aldrich, USA) used were 1:16,000 diluted anti-rabbit, 1:8000 diluted anti-mouse or 1:8000 diluted anti-goat. All antibodies were diluted in 1% milk in PBS-T. An ECL-plus chemiluminescent kit (GE Healthcare, UK) and Fujifilm luminescent image analyser (LAS 4000 Version 2.0) were used to capture the signals. After detection of each target, membranes were stripped, re-probed with anti-GAPDH antibody as described in Section 2.4. Intensities of each target were normalised against that of GAPDH in respective wells and values expressed in densitometric units.

2.8. Effect of TNF-α treatment on Cx43 and dye uptake in CHME-5 cells

TNF-α has been shown to be one of main downstream effectors of the AGE–RAGE pathway and/or microglial activation. To confirm that TNF-α induces increased expression of Cx43 in CHME-5 cells, CHME-5 cells were treated with 10 ng of TNF-α for 6 and 24 h. Cell lysates were processed for the detection of Cx43 using western blot methods as described in Sections 2.4 and 2.7; a high-resolution 15% SDS PAGE gel was used for this part. To investigate increased functional Cx43 coupling and/or hemichannels, dye uptake assays using Lucifer yellow and propidium iodide were performed as described below.

2.8.1. Dye uptake assay

The assays were modified from published studies (Becker and Green, 2002; O'Carroll et al., 2008). For dye uptake/influx assays, cells were grown on cover slips, in 24-well plates as described in Section 2.4. Cells were cultured in four groups (a. Control, b. TNF-α only, c. TNF-α + Carbenoxolone and d. TNF-α + Lanthanam Chloride) with two sets (set I: Lucifer yellow, set II: propidium iodide). When cells were more than 90% confluent, cells (except controls) were treated with 10 ng TNF-α. At the end of 6 h, 100 μM Carbenoxolone (Cbx) and 200 μM Lanthanam chloride ($LaCl_3$) were added in groups c and d respectively. Cbx and $LaCl_3$ are GJC/hemichannel blockers (O'Carroll et al., 2008). After 5 min of incubation with Cbx and $LaCl_3$ at 37 °C under 5% CO_2, a clean scrape was made in all groups in set I and 1% Lucifer yellow (LY) dye was added. In set II, 2 mM propidium iodide (PI) was added. Controls were supplemented with vehicles; DMSO for set I and PBS for set II. After 30 minute's incubation at 37 °C, cells were washed with PBS, fixed with 4% PFA, stained with Hoechst 33258 nuclear dye (Molecular Probes, Invitrogen, USA; 1:500 diluted in PBS) for 5 min, washed with PBS and coverslips mounted with prolong gold mounting medium (Molecular Probes, USA). Images were collected using a Leica DMR microscope.

2.9. Effect of neutralising TNFRII on Cx43 expression

CHME-5 cells were grown in complete DMEM-F12 with 10% FBS and conditions as described in Section 2.1. Cell numbers were adjusted to reach confluency in 24 h in a 25 cm^2 culture flask (CELLSTAR®, Greiner Bio-One, Germany). Cells were assigned to five treatment groups; a: Untreated control, b: Cells treated with 10 ng TNF-α, c: Cells pre-incubated with 0.1 μg of anti-TNFRII neutralising antibody (MAB226, R& D Systems Inc, USA) + 10 ng TNF-α, d: Cells pre-incubated with 1.0 μg of anti-TNFRII antibody + 10 ng TNF-α, e: Cells pre-incubated with 10 μg of anti-TNFRII antibody + 10 ng TNF-α. Pre-incubation with TNFRII neutralising antibody was done for 4 h (in c, d and e), followed by TNF-α treatment (10 ng) for 6 h (b, c, d and e). At the end of the treatment period, cells were washed with PBS, cell lysates collected using RIPA lysis buffer and processed for detection of Cx43 protein using western blot as described in Section 2.7.

3. Statistical analysis

Data from three independent experiments were used for analysis. Means of various treatment groups were compared using one-way-ANOVA (Prism software, version 3.02, GrapPad Inc, USA) and Tukey's post hoc test (for multiple comparisons) was carried out to determine if the differences between means were statistically significant. $P < 0.05$ was considered to be a significant difference. Data were expressed as the mean ± standard deviation.

4. Results

4.1. Human microglial cells (CHME-5) are activated by extracellular AGEs

Immunocytochemical results using two well-known microglial markers showed that CHME-5 cells are activated in response to exogenous AGEs (Fig. 1). Glut-5 was detected in CHME-5 cells in both controls (untreated cells and BSA treated cells) and AGEs-treated cells; the levels increased with increasing dose of AGEs (Fig. 1A, red). CR3/43 (microglial activation marker) staining was negligible in controls and showed an increase in immunostaining with increasing dose of AGEs, in AGE-treated cells (Fig. 1A, green). Western blot performed for CR3/43, using cell lysates from controls and cells treated with three doses of AGEs showed a significant, dose-dependent, increase in the intensity of the CR3/43 positive 30 kDa band. This band was not detected in controls (Fig 1, B and C).

4.2. Increased expression of 55 kDa, glycosylated RAGE in AGEs-treated CHME-5 cells

The antibody used for RAGE detected three bands on Western blots in the CHME-5 cells; 50, 55 and approximately 60 kDa bands corresponding to the sizes of the non-glycosylated and two N-glycosylated full length RAGE proteins respectively (Lue et al., 2005; Osawa et al., 2007; Park et al., 2011) (Fig. 2A). The intensity of the non-glycosylated 50 kDa band increased significantly in response to exogenous AGEs and decreased when AGEs–RAGE interaction was inhibited the presence of anti-RAGE Fabs, however the decrease in the 50 kDa band was not significant (Fig. 2B). The 55 kDa band corresponding to glycosylated RAGE showed a dramatic 6.5-fold increase upon treatment with AGEs compared to untreated controls, and a significant drop in the level upon inhibition of AGEs–RAGE interaction in the presence of anti-RAGE Fabs (Fig. 2A and C). The levels of the 50 and 55 kDa bands were not significantly different in cells treated with anti-RAGE Fabs only compared to controls (Fig. 2A, B and C). Interestingly the band at ~60 kDa, also representing a form of glycosylated RAGE (Park et al., 2011), did not show any significant change in intensity, irrespective of the treatment (Fig. 2A and D). The total levels of RAGE (combined intensities of all RAGE positive bands) were significantly increased in response to AGEs and dropped in cells treated with anti-RAGE Fabs + AGEs. The levels of total RAGE were not different in cells treated with anti-RAGE Fabs only compared to controls (Fig. 2A and E). There was no significant change in RAGE for all

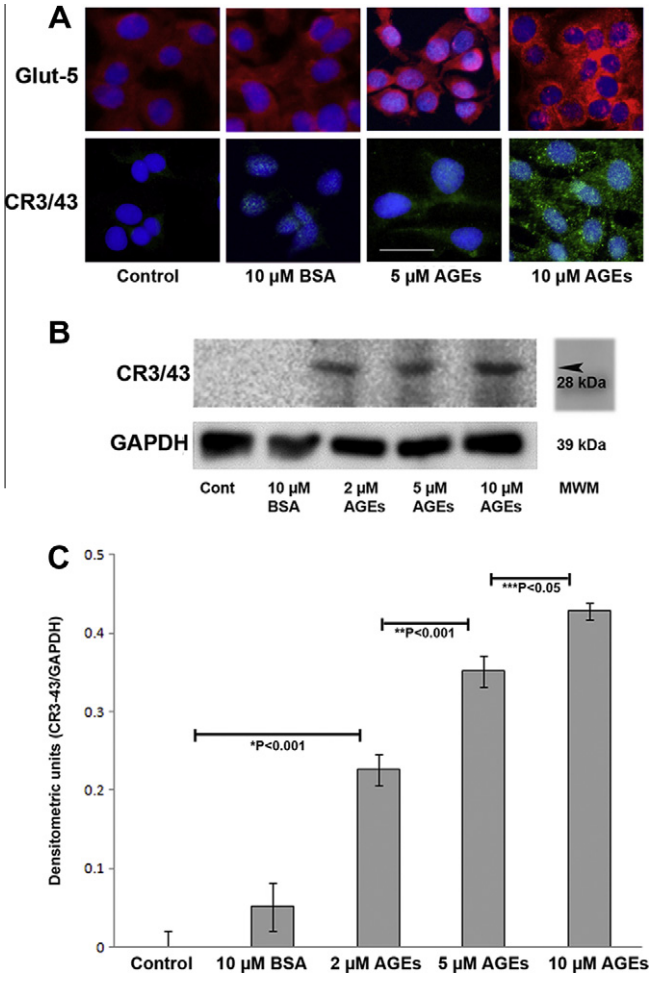

Fig. 1. Detection of microglial activation. Representative photomicrographs (A) showing immunostaining of human microglial CHME-5 cells using anti-Glut-5 (top panel, red) and anti-CR3/43 (HLA-DR/DP/DQ, bottom panel, green) antibodies in control (untreated) and cells treated with 10 μM BSA or one of two different doses (5 and 10 μM) of AGEs for 24 h. Both markers showed increases in immunostaining with increasing doses of AGEs, compared to control and BSA treated cells. Representative western blot for the marker CR3/43 (B) and corresponding histogram (C) show a significant dose-dependent increase in the intensity of CR3/43 band in cells treated with three doses of AGEs (2, 5 and 10 μM). Results shown are representative of three independent experiments. All images are of the same magnification. Scale bar in A: 50 μm. *P: significance between control and 2 μM AGEs, **P: significance between 2 and 5 μM AGEs, ***P: significance between 5 and 10 μM AGEs. (For interpretation of the references to colour in this figure legend, the reader is referred to the web version of this article).

isoforms between AGEs only treated cells and cells pre-incubated with Ms Fabs, followed by AGEs treatment (Fig. 2), suggesting that Ms Fabs did not affect antibody binding and that the effects of anti-RAGE Fabs were specific. There was no difference in the total levels of RAGE between untreated cells and cells treated with 10 μM BSA (Fig. 2F), suggesting that the increased RAGE levels were induced specifically by AGEs.

4.3. CHME-5 cells release TNF-α in response to AGEs

Conditioned media obtained from CHME-5 cells treated with 10 μM AGEs and/or pre-incubated with 10 μg non-immune Ms Fabs, prior to treatment with AGEs showed 43 and 52 pg of TNF-α/gm of total cellular protein respectively, compared to undetected levels in media obtained from untreated cells (Fig. 3). The secreted TNF-α levels/gm of total protein dropped 4.3-fold in cells treated with 5 μg anti-RAGE Fabs + AGEs compared to AGEs only treated cells. TNF-α levels could not be detected in the media collected from cells pre-incubated with 10 μg anti-RAGE Fabs + AGEs, anti-RAGE Fabs only or cells treated with 10 μM BSA only (Fig. 3). TNF-α levels followed the same pattern when expressed in pg/ml of the media.

4.4. TNFRII is expressed in abundance on human microglia compared to TNFRI

The basal level of TNFRI was negligible in untreated control cells in the amount of total protein (15 μg) loaded (Fig. 4A), but the level increased significantly in cells supplemented with 10 μM AGEs. When the AGEs–RAGE interaction was inhibited by the addition of two different doses of anti-RAGE Fab fragments, there was a decrease in TNFRI levels but this was not significant (Fig. 4A and C). The basal level of TNFRII in untreated control CHME-5 cells was 2.2-fold higher than TNFRI. The level of TNFRII increased significantly upon treatment with AGEs, and these levels decreased significantly to the basal level when AGEs–RAGE interaction was inhibited in the presence of anti-RAGE Fabs (Fig. 4B and C). The levels of both TNFRI and TNFRII in cells treated with AGEs only and cells pre-incubated with Ms Fabs prior to AGEs treatment, did not alter significantly. In addition, the levels of TNFRI and TNFRII in cells supplemented with anti-RAGE Fabs only were similar to untreated controls (Fig. 4A, B and C) and cells treated with only BSA (Fig. 4D, data shown for TNFRII only). These results (Sections 4.3 and 4.4) indicate that TNF-α is released extracellulary into the medium and that TNFRs levels, especially TNFRII, increase in response AGEs–RAGE interaction in CHME-5 cells.

4.5. Connexin43 (Cx43) is a downstream effector of AGEs–RAGE interaction in human microglial CHME-5 cells

Western blots showed two bands positive for Cx43 between 43 and 46 kDa, and a faint band at 51 kDa. The bands between 43 and 46 kDa correspond to the non-phospho (NP) and phosphoforms (P) of Cx43 (Pahujaa et al., 2007; Saez et al., 1998; Solan and Lampe, 2007), while the identity of the 51 kDa band is not known. These bands (43–46 kDa) showed a significant increase in their intensities in cell lysates obtained from cells treated with 10 μM AGEs and cells treated with 10 μg Ms Fab + 10 μM AGEs, compared to untreated controls (Fig. 5A and B). The intensity of both bands at 43–46 kDa decreased significantly when the AGEs–RAGE interaction was blocked using two doses of anti-RAGE Fabs (Fig. 5A and B); this decrease was more marked in cells where 10 μg anti-RAGE Fab was used. Interestingly, the intensity of the Cx43 positive bands was significantly reduced in cells supplemented with 10 μg anti-RAGE Fabs only compared to untreated controls, suggesting that blocking RAGE may have some non-AGEs-mediated effects on the expression of Cx43. There was no difference in the intensity of Cx43 bands between untreated cells and cells treated with BSA only (Fig. 5C). These results support the notion that Cx43 is a downstream effector of AGEs–RAGE mediated pathways in human microglial CHME-5 cells.

4.6. TNF-α induces increased Cx43 expression and dye uptake and blocking TNFRII inhibits Cx43 expression in a dose-dependent manner in CHME-5 cells

To confirm the induction of Cx43 by the TNF-α released as a result of AGEs–RAGE interaction and/or microglial activation, CHME-5 cells were treated with 10 ng of TNF-α for 6 and 24 h. The results showed that TNF-α induces a time-dependent increase in the levels of Cx43 in CHME-5 cells (Fig. 6A). An interesting observation on this high resolution PAGE-western blot was that untreated controls showed a faint (negligible) additional band at 51 kDa and the

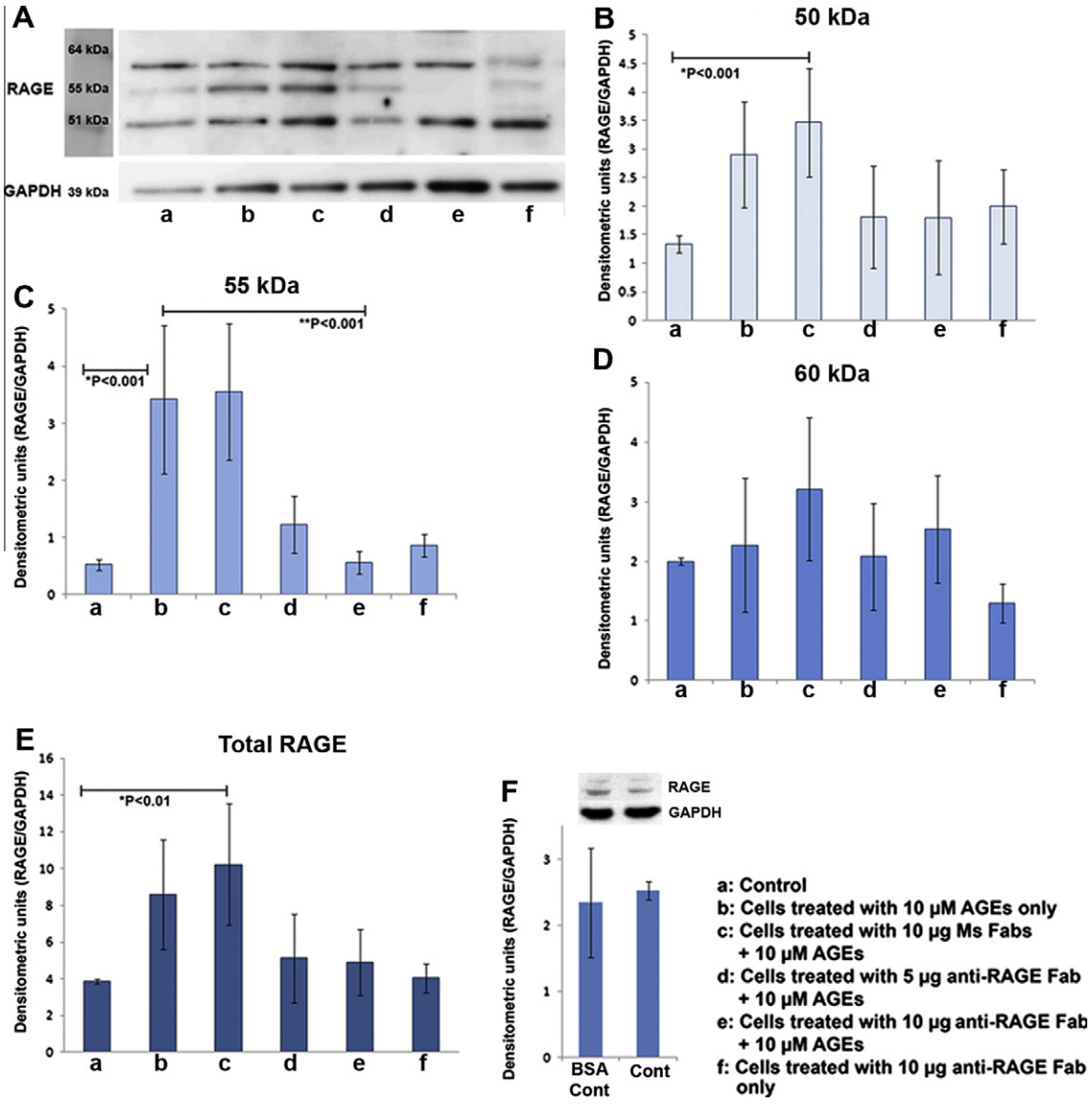

Fig. 2. RAGE isoforms in CHME-5 cells in response to AGEs treatment. Representative immunoblot (A) and histograms (B, C, D, E and F) showing the levels of various RAGE proteins isoforms observed in the CHME-5 cells treated with 10 μM AGEs in the absence and presence of two different doses of anti-RAGE Fab fragments. Controls included untreated CHME-5 cells, cells treated with AGEs + 10 μg of mouse (Ms) Fabs, 10 μM BSA or 10 μg anti-RAGE Fabs only. Immunoblot detected three bands at 50, 55 and 60 kDa, corresponding to the full-length un-glycosylated and two differentially N-glycosylated bands respectively (A). Both 50 and 55 kDa bands showed significant increases in intensity levels in response to AGEs (B and C). The levels dropped when the AGEs–RAGE interaction was blocked using two different doses of anti-RAGE Fabs, however the decrease was significant only in the 55 kDa band (C). The 60 kDa band did not change significantly upon treatment (D). The combined levels of all RAGE positive bands followed a similar pattern to those of 50 and 55 kDa (E) with no change between untreated controls and cells treated with 10 μM BSA only (F). GAPDH was used as a loading control and values for each target protein were normalised with the values of GAPDH in the respective wells and expressed in densitometric units. Results shown are representative of three independent experiments and each column represents the mean and standard deviation of the combined data. a: untreated control, b: cells treated with 10 μM AGEs, c: Cells pre-incubated with 10 μg Ms Fabs + 10 μM AGEs, d: Cells pre-incubated with 5 μg anti-RAGE Fabs + 10 μM AGEs, e: Cells pre-incubated with 10 μg anti-RAGE Fabs + 10 μM AGEs, f: Cells treated with 10 μg anti-RAGE Fabs only. *P shows a significant difference between a and c/a and b. **P shows a significant difference between b and e.

intensity of this band increased upon TNF-α treatment along with other bands observed between 43 and 46 kDa (Fig. 6A). The 51 kDa band was specifically induced by TNF-α.

Cells treated with 10 ng TNF-α for 6 h also showed increased spread of the dye Lucifer yellow (LY) from the site of scrape injury to neighbouring cells. LY can pass through opened GJC in cells connected by GJC (Eugenin et al., 2001). In untreated controls, LY was restricted to the site of injury (Fig. 6B). The dye-influx assay using propidium iodide (PI), a dye that can pass through open hemichannels (O'Carroll et al., 2008), showed dramatic uptake of PI in TNF-α treated cells compared to untreated control. This uptake was completely inhibited in cells pre-incubated with GJC/hemichannel blockers Cbx and $LaCl_3$ (Fig. 6C).

We also investigated the effect of neutralising TNFRII on Cx43 expression in cells treated with 10 ng TNF-α for 6 h. As seen earlier, TNF-α treatment induced increased Cx43 expression compared to untreated cells. There was a dose-dependent drop in the intensity of Cx43 bands when cells were pre-incubated with three different doses (0.1, 1.0 and 10 ng) of monoclonal TNFRII neutralising antibody followed by TNF-α treatment (Fig. 6D).

The similar effects of AGEs and AGEs + mouse (Ms) Fabs on targets (RAGE, Cx43, TNF-α and TNF-receptors) and the reduction of

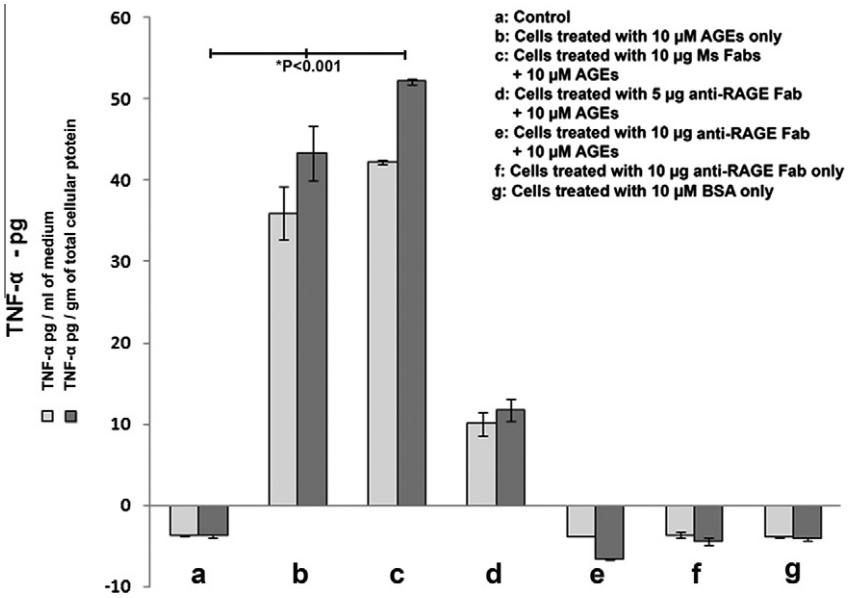

Fig. 3. TNF-α levels. Histogram showing the levels of TNF-α using the ELISA method. Levels were expressed in both pg of TNF-α/ml of media and pg of TNF-α/gm of total cellular protein; both showed a similar pattern. Untreated controls (a) showed negligible amounts of the cytokine TNF-α, whereas cells treated with 10 μM AGEs (b) or cells pre-incubated with 10 μg Ms Fabs followed by treatment with 10 μM AGEs (c) showed 43 and 52 pg of TNF-α released in media/gm of total cellular protein respectively. Pre-incubation with 5 μg of anti-RAGE Fabs followed by AGE treatment (d) showed a significant 3.5–4.3-fold decrease in TNF-α levels compared to b and c. Levels of TNF-α were undetectable in cells pre-incubated with 10 μg anti-RAGE Fabs + 10 μM AGEs (e), cells treated with10 μg anti-RAGE Fabs only (f) or cells treated with 10 μM BSA only (g). *P shows a significant difference between a, b and c. Results shown are representative of three independent experiments and each column represents the mean and standard deviation of the combined data.

some of these in the presence of AGEs + anti-RAGE Fabs or TNF-α + TNFRII antibody suggests that anti-RAGE Fabs/anti-TNFRII antibodies bind specifically to RAGE/TNFRII respectively; mouse IgGs did not show any non-specific reactivity. The similar results obtained between untreated controls and BSA only treated cells also suggest that the effects observed in this study are specifically due to the glycated BSA (AGEs) and not due to any non-specific molecular crowding of BSA. We did not therefore perform the controls using Ms Fabs or BSA while testing the effects of monoclonal TNFRII neutralising antibody on Cx43 expression.

5. Discussion

Previous studies using microglia/macrophages of animal origin show evidence that AGEs activate microglia. Studies using human microglia are however sparse with only one report showing AGEs-induced ROS generation in human microglia. Differences exist between microglia of human and rodent origin especially in the way they respond to some stimuli and this, coupled with the fact that AGEs-mediated effects can be cell type specific (Colton et al., 1996; Dragunow, 2008; Schmitt et al., 2006) warrants further investigation. We therefore sought to determine the effects of exogenous AGEs on microglia of human origin and investigate the downstream effectors during the process of activation. There are some studies reporting AGEs-mediated activation of mitogen-activated protein kinases (MAPK), nuclear factor kB (NF-kB) and macrophage-colony stimulating factor (M-CSF) in rodent macrophages, BV2 microglial cell line and retinal microglia (Neumann et al., 1999) and Aβ–RAGE mediated activation of M-CSF in human primary microglia (Lue et al., 2001; Wang et al., 2007). However, to the best of our knowledge, ours is the first study reporting TNF-α, TNF-receptors (especially TNFRII) and connexin43 as downstream effectors of AGEs–RAGE interaction in microglia of human origin.

The availability of human tissue, low yield of human microglia and ethical issues associated with the use of human tissue pose significant challenges for establishing primary human microglial cell cultures. Most of the available microglial cell lines of human origin (HMO6, C13-NJ, CHME-3 and CHME-5) were obtained from embryonic foetal human microglia through viral transformation (retroviral vector encoding v-myc/SV-40 large T antigen) (Atanassov et al., 1995; Janabi et al., 1995; Nagai et al., 2001; Peudenier et al., 1991). We received a well-characterised CHME-5 cell line, originally established by Janabi et al. (1995) (Janabi et al., 1995), as a gift from Professor Pierre Talbot (Laboratory of Neuroimmunovirology, INRS-Institute, Armand-Frappier, Canada). These cells express the antigens present on adult human microglia, secrete inflammatory cytokines upon activation, exhibit some properties of primary human microglia and have been used previously by us (Shaikh and Nicholson, 2009) and others (Atanassov et al., 1995; Bigl et al., 2008; de Gannes et al., 1998; Schmitt et al., 2006). It is thought that cell lines obtained through viral transformation loose their properties over the number of passages; however, we used CHME-5 cells from very early passages (p11–p15) in this study. We therefore believe that these cells retained their microglial properties.

The cellular effects of AGEs not only depend on the degree of modification and special structures within the modified protein but also on the cell types on which they act; AGEs can induce cell death in some cells, and cell-proliferation in others (Schmitt et al., 2006). We did not observe increased cell death in CHME-5 cells supplemented with AGEs compared to controls (data not shown), indicating that AGEs do not induce accelerated cell death in CHME-5 cells at the doses used in this study. In agreement with work done in rodents (Munch et al., 1998; Schmitt et al., 2006; Wong et al., 2001), we showed that human microglial CHME-5 cells are activated in the presence of exogenous AGEs in a dose-dependent manner. AGEs are a heterogeneous population of highly reactive molecules, able to bind to specific receptors present on the cell surface and initiate signal transduction pathways. Several AGE-binding proteins have been identified to date (Schmitt et al., 2006), however the most characterised signal transduction receptor for

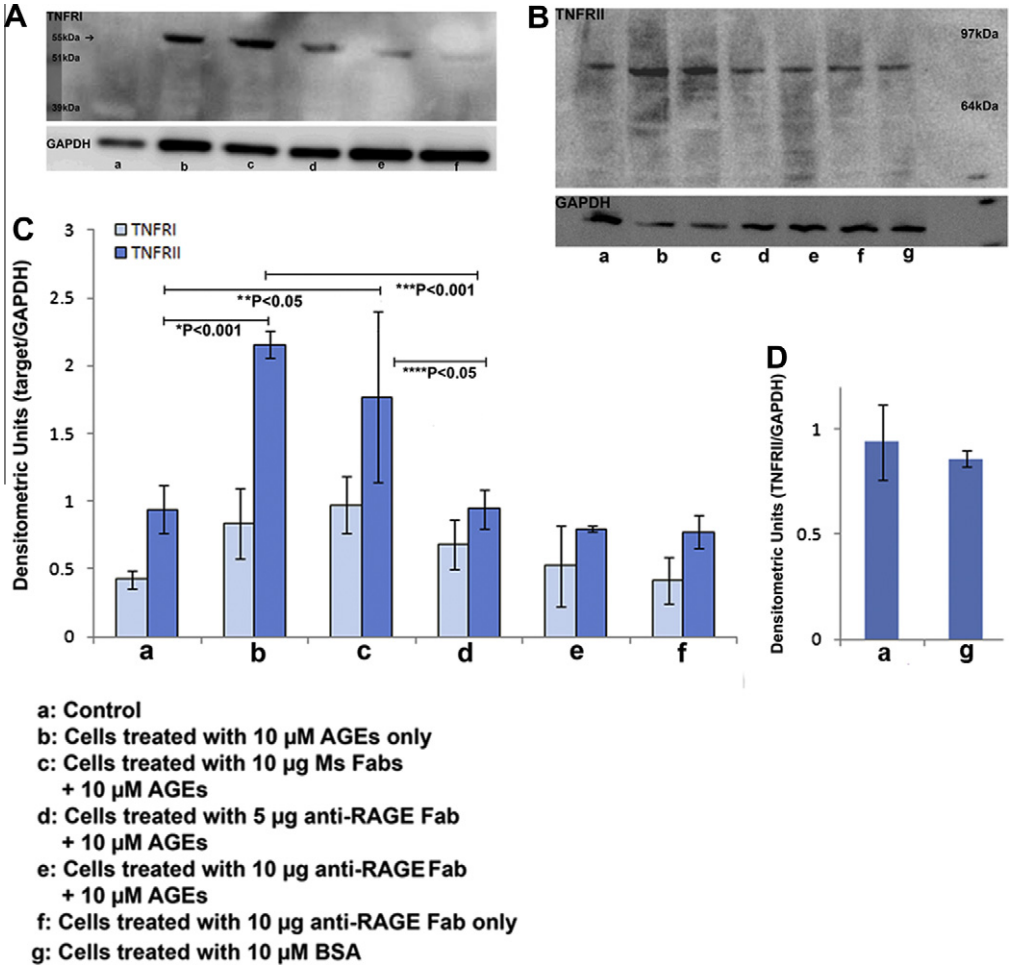

Fig. 4. Levels of TNF-α receptors (TNFRI and TNFRII). Representative immunoblots showing the bands positive for TNFRI (A, 55 kDa) and TNFRII (B, 75 kDa) in the CHME-5 cells treated with AGEs in the absence and presence of two different doses of anti-RAGE Fab fragments. The levels of TNFRI were negligible in the untreated controls (a), and increased in cells treated with 10 μM AGEs (b) or cells pre-incubated with 10 μg Ms Fabs followed by treatment with 10 μM AGEs (c) (A and C); the levels of TNFRI dropped in the presence of two doses of anti-RAGE Fabs (d and e respectively) and cells treated only with anti-RAGE Fabs (f) (Figure A and C). The basal levels of TNFRII levels were at least two fold higher than TNFRI, and increased dramatically in response to AGEs with a decrease in the presence of anti-RAGE Fab fragments (B and C). The levels of TNFRII were not different between control (a) and cells treated with 10 μM BSA (g) (D). GAPDH was used as a loading control and values of target proteins were normalised with the values of GAPDH in the respective wells and expressed in densitometric units. a: untreated control, b: cells treated with 10 μM AGEs, c: Cells pre-incubated with 10 μg Ms Fabs + 10 μM AGEs, d: Cells pre-incubated with 5 μg anti-RAGE Fabs + 10 μM AGEs, e: Cells pre-incubated with 10 μg anti-RAGE Fabs + 10 μM AGEs, f: Cells treated with 10 μg anti-RAGE Fabs only, g: Cells treated with 10 μM BSA. $^{*}P$ shows significant difference between a and b of TNFRII, $^{**}P$ shows the significance in means between a and c of TNFRII, $^{***}P$ shows the significant difference between b and d of TNFRII, $^{****}P$ shows the significant difference between c and d of TNFRII. Results are representative of three independent experiments and each column represents the mean and standard deviation.

AGEs is RAGE (Receptor for AGEs); the presence of RAGE has been shown on microglia in human brain as well as other cells of animal and human origin (Lue et al., 2001, 2005; Schmitt et al., 2006; Yan et al., 1998). Studies showing RAGE–Aβ mediated activation of NF-kB and MAPK in microglia and macrophages of rodent origin (Yan et al., 1996, 1998) have been reported, while others have shown AGEs-mediated NF-kB activation in murine macrophages (Neumann et al., 1999). Schmitt et al. (Schmitt et al., 2006) speculated that RAGE and/or other AGEs-receptors may be involved in AGEs-mediated effects on human microglial cells, however no such role for RAGE or any other AGEs-receptors has been confirmed experimentally in microglia of human origin.

In this study, we showed that CHME-5 cells express full-length un-glycosylated (50 kDa) and two glycosylated isoforms of RAGE (55 and 60 kDa). Although the levels of unglycosylated and the 55 kDa glycosylated form of RAGE increased in the presence of AGEs, the most dramatic change was observed in glycosylated 55 kDa RAGE. RAGE exists in several isoforms and expression is cell type specific (Gefter et al., 2009; Osawa et al., 2007; Park et al., 2011). The size of these isoforms depends on differential transcript splicing, the type of glycans involved in N-glycosylation and the number of sites glyocosylated. Each of these isoforms play a regulatory role in the patho-physiological functions of RAGE, ligand recognition and cellular responses (Osawa et al., 2007). So far, two N-glycosylation sites have been identified in RAGE protein; the site within V domain is shown to be important in AGEs-ligand recognition (Osawa et al., 2007). In addition, Park et al. (Park et al., 2011) recently reported that the 59 kDa isoform is modified by high mannose/hybrid glycans, whereas the smaller protein species of RAGE (~57 kDa) is modified by complex glycans. The findings of these studies and our observations of dramatic changes in the 55 kDa RAGE isoform in the presence of AGEs suggest that glycosylation of RAGE within the V-domain by complex glycans may be necessary for mediating AGEs effects in CHME-5 cells. RAGE shows a positive feedback in the presence of ligands (Lue et al., 2005). This can explain the increased levels of endogenous RAGE

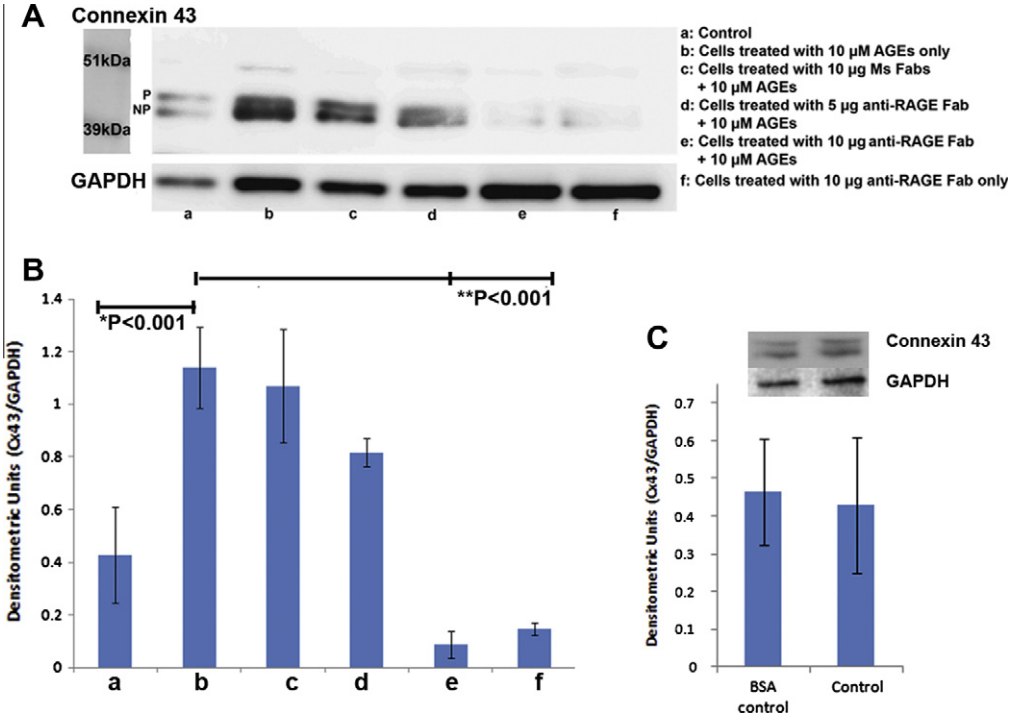

Fig. 5. Cx43 expression in CHME-5 cells in response to AGEs and anti-RAGE Fabs. Representative immunoblot (A) showing the Cx43 isoforms identified using a polyclonal anti-Cx43 antibody in CHME-5 cells treated with 10 μM AGEs (b) in the absence and presence of either 10 μg Ms Fabs (c) or two different doses (5 and 10 μg) of anti-RAGE Fab fragments (d and e respectively). Controls included untreated CHME-5 cells (a) and cells treated with 10 μg of anti-RAGE Fabs only (f) or 10 μM BSA only. The antibody used identified two bands between 43 and 46 kDa representing non-phospho (NP) and phosphoforms of Cx43 (A). These bands showed significant increases in response to AGEs and a dose-dependent (significant) drop in the levels of Cx43 observed when AGE–RAGE interaction was blocked in the presence of two doses of anti-RAGE Fab fragments (B). The Cx43 levels in cells treated with 10 μg anti-RAGE Fab fragments in the presence or absence of AGEs (e and f) were significantly reduced compared to controls (a) (B). The levels of Cx43 were not different between untreated controls and cells treated with BSA only (C). An additional faint band at 51 kDa, positive for Cx43, was also observed in CHME-5 cells (A). GAPDH was used as a loading control and values for target protein were normalised with the values of GAPDH in the respective wells and expressed in densitometric units. Results shown are representative of three independent experiments and each column represents the mean and standard deviation of the combined data. *P: difference between a and b, **P: difference between b, e and f.

in the presence of AGEs and the decrease in its levels when AGEs–RAGE interaction was blocked by anti-RAGE Fabs and AGEs were unable to maintain the positive feedback.

We also observed that human microglial CHME-5 cells expressed the gap junction protein connexin43 (Cx43). Two bands positive for Cx43 were observed between 43 and 46 kDa representing non-phospho and a phosphoform of Cx43 (Pahujaa et al., 2007; Saez et al., 1998; Solan and Lampe, 2007). A faint band was also observed at 51 kDa; the identity of this band has not been reported in the literature. AGEs induced an increase in the expression of Cx43 (both bands between 43 and 46 kDa) in human CHME-5 cells. A significant dose-dependent decrease in Cx43 in the presence of anti-RAGE Fab + AGEs suggests Cx43 is one of the downstream effectors of the AGEs–RAGE pathway in CHME-5 cells. AGEs activate microglia and activated microglia of both human and rodent origin have been shown to release a cocktail of pro-inflammatory cytokines (Munch et al., 2003; Wang et al., 2007). In agreement with these studies, the present study also showed release of TNF-α by human microglial CHME-5 cells in response to AGEs-mediated activation. Until recently, it was thought that microglia did not express Cx43, however, researchers have now demonstrated that rodent microglia (both primary cells and cell lines) and human monocytes not only express Cx43 but also form functional coupling when treated with TNF-α alone or in combination with IFN-γ (Eugenin et al., 2003, 2001, 2007; Garg et al., 2005), indicating that when a critical threshold of cell activation is reached under the influence of a combination of stimuli, microglia can form gap junction channels (GJCs). GJCs facilitate cell–cell communication and mediate the transfer of molecules involved in signal transduction. GJCs are formed by joining of two adjacent hemichannels from neighbouring cells; each hemichannel is composed of six protein subunits called connexins. There are at least 20/21 human connexins known to date, and the properties of these channels in terms of the passage and type of molecules depend on the connexin subunit composition of the hemichannels (Kielian, 2008). The major connexin subunit observed in the CNS is Cx43 (Altevogt and Paul, 2004; Dermietzel et al., 2000; Rash et al., 2001) expressed mainly in astrocytes. The main stimuli that can influence Cx43 expression are the cytokines TNF-α, IL-1β, IFN-γ, IL-6 and NO, all released as a result of microglial activation. Although cytokines rarely work in isolation, TNF-α appears to be the primary mediator of Cx43 expression (Eugenin et al., 2003, 2001; Vandamme et al., 2004). Altered levels of Cx43 and GJC coupling has been associated with several neuroinflammatory conditions (Eugenin et al., 2007; Fonseca et al., 2002; Kielian, 2008) and microglia, being the innate immune effector cells of the CNS, contribute significantly to neuroinflammation.

In agreement with previous studies on activation of other cell types (Eugenin et al., 2003, 2001; Vandamme et al., 2004), we also found increased levels of TNF-α released by CHME-5 cells in response to AGEs. In addition, TNF-α not only induced increased Cx43 expression in CHME-5 cells, but we were able to show the transfer of Lucifer yellow dye from the site of scrape injury to neighbouring cells and uptake of propidium iodide (PI) by these cells. The uptake of PI was completely inhibited in the presence of GJC/hemichannel blockers. These results indicated that the increased Cx43 protein observed in AGEs and/TNF-α treated CHME-5 cells could be in part contributing to the functional coupling/

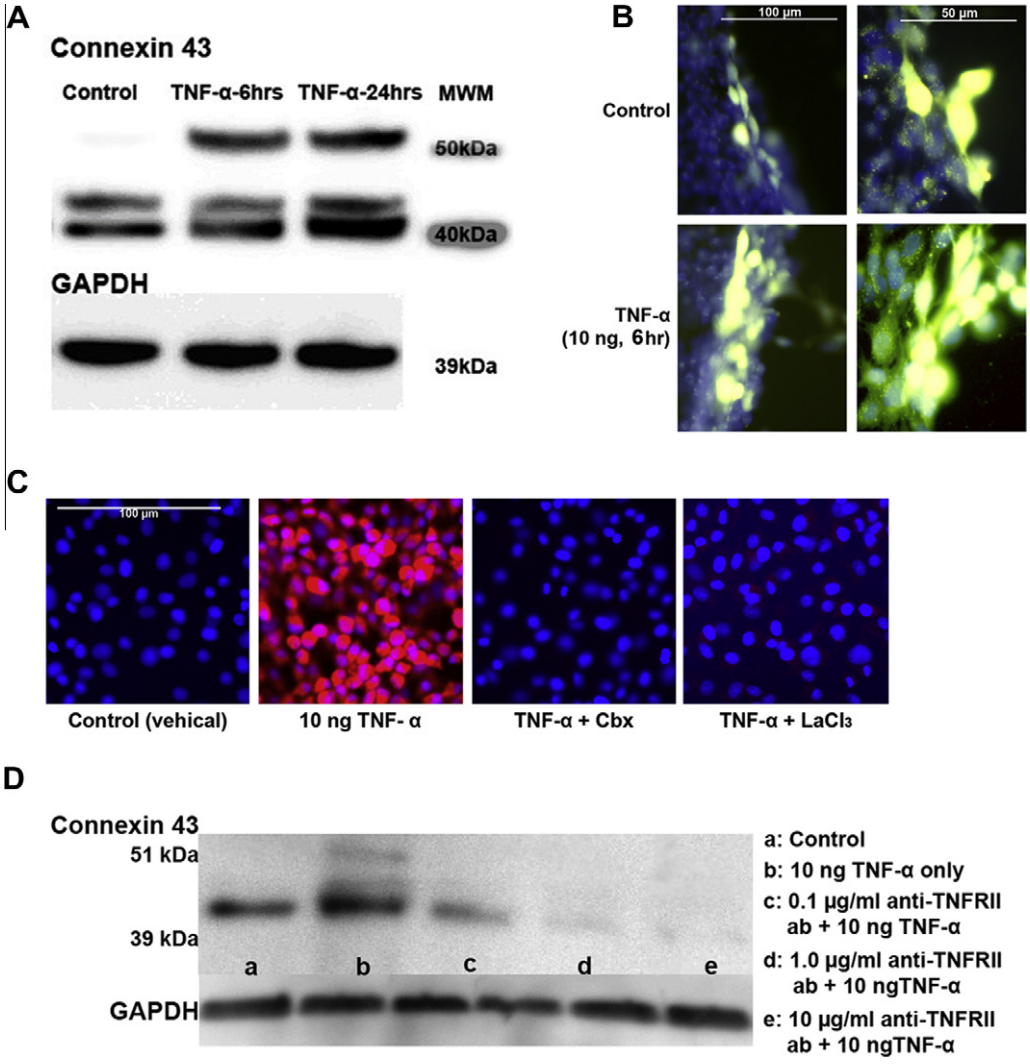

Fig. 6. TNF-α induced Cx43 expression and dye uptake in CHME-5 cells and the effect of neutralising TNFRII on Cx43. A. Representative immunoblot showing the bands between 43 and 46 kDa and 51 kDa positive for Cx43 using a specific anti-Cx43 polyclonal antibody, in CHME-5 cells treated with 10 ng of TNF-α for 6 and 24 h. GAPDH was used as a loading control. TNF-α induced a time-dependent increase in all the bands positive for Cx43 (43–46 kDa and 51 kDa) compared to controls; the 51 kDa band was induced only in the presence of TNF-α. MWM; molecular weight marker. B. Photomicrograph representing the spread of the Lucifer yellow dye to neighbouring cells from the site if scrape injury in cells treated with 10 ng of TNF-α for 6 h (bottom row), whereas the dye was restricted to a few cells at the site of injury in untreated cells (top row). Second column shows magnified images. Scale bar in Column 1 is 100 µm and in Column 2 is 50 µm. C. Photomicrograph showing the dye-influx assay using Propidium iodide (PI). Cells treated with 10 ng TNF-α for 6 h showed dramatic uptake of PI compared to no dye uptake in untreated controls. This uptake was completely inhibited when cells where incubated with GJC/hemichannel blockers Cbx and $LaCl_3$. D. Immunoblot showing the increase in the intensity of Cx43 positive bands in cells treated with 10 ng TNF-α for 6 h(b) compared to control (a). This increase in Cx43 band showed a dose-dependent drop when cells were pre-incubated with 0.1, 1.0 and 10 µg of monoclonal TNRII neutralising antibody (c, d and e respectively). Results are representative of three independent experiments.

active hemichannels in these cells. Although Wang et al., (Wang et al., 2011) recently reported AGEs-mediated down regulation of Cx43 in human aortic endothelial (HAES) cells, ours is the first report showing experimentally, increased Cx43 expression in activated human microglial CHME-5 cells and functional coupling of these cells following AGEs–RAGE interaction. Closing and opening of GJCs in cells also depend on the post-transcriptional phosphorylation state of Cx proteins, with Cxs presenting several sites for phosphorylation by many kinases (Pahujaa et al., 2007; Saez et al., 1998). Based on the status of phosphorylation, NP (non-phosphoform), P1, P2, P3 phosphoforms of Cx43 have been identified. We observed two bands between 43 and 46 kDa representing the non-phospho and phosphoforms of Cx43. The levels of both bands increased in the presence of AGEs, however we did not observe changes in any particular form of Cx43 upon AGEs treatment. An interesting observation was that the drop in the levels of Cx43 was much more dramatic when RAGE was inhibited using anti-RAGE fragments than the increase observed in the presence of AGEs only, suggesting that alteration in the Cx43 expression could be the result of the interaction of RAGE not only with AGEs but with other ligands as well. We also observed an additional faint band at 51 kDa, and interestingly this band was observed to be specifically induced when CHME-5 cells were treated with exogenous TNF-α; the intensity of this band was similar to other Cx43 positive bands. The identity of this band is not known. We cannot comment as to whether this band is unprocessed Cx43 or a result of some post-transcriptional modification and/or cross-reaction of Cx43 with other proteins, since such modifications of Cx43 is not reported in the literature.

The effect of pro-inflammatory cytokines, especially TNF-α and IL-1β, on GJCs has been reported to be highly cell type specific. TNF-α has been demonstrated to down-regulate Cx43 expression in heart after injection of bacterial endotoxin, whereas injections of endotoxins in kidney and lung resulted in up-regulation of

Cx43 (Brosnan et al., 2001). Similarly, TNF-α can have differential effects on Cx43 expression in endothelial cells, astrocytes and microglia (Wang et al., 2011) (Kielian, 2008). We confirmed in our study that, TNF-α increased the levels of Cx43 protein in human microglial CHME-5 cells and these cells were functionally coupled.

TNF-α exerts its effects via two receptors; 55 kDa TNFRI and 75 kDa TNFRII. We therefore analysed the levels of these two receptors in the human microglial CHME-5 cells upon AGEs treatment in the absence and presence of two different doses of anti-RAGE Fab fragments. Levels of both receptors increased in the presence of AGEs and the levels dropped in the presence of anti-RAGE Fab. Interestingly, the change seen in TNFRI expression was minimal, whereas TNFRII showed a dramatic increase upon AGEs treatment. In addition, neutralising TNFRII using neutralising antibody inhibited TNF-α induced increase in the Cx43 levels. We propose that the AGEs-induced release of TNF-α by the CHME-5 cells, can have both autocrine and paracrine effects on CHME-5 cells via its receptors. TNF-α has been shown to induce microglial proliferation (Dopp et al., 2002; Thery and Mallat, 1993). TNFRI is known to induce cleavage of caspases and activate apoptotic cascades whereas TNFRII signals primarily activate the NF-kβ pathway and has been shown to up-regulate protective proteins such as Mn-Superoxide Dismutase (MnSOD) that counteracts the apoptotic signals (Dopp et al., 2002). In the present study, the dramatic increase in TNFRII and Cx43 observed in CHME-5 cells upon treatment with AGEs, increased dye uptake and inhibition of Cx43 upon blocking TNFRII suggest a significant role for TNFRII and both GJC and hemichannels in propagating the downstream affects of AGE–RAGE interaction in CHME-5 cells.

6. Conclusions

We have shown experimentally Cx43 as a downstream effector of AGEs–RAGE interaction in human microglial CHME-5 cells. From our results, it is likely that AGEs-mediated microglial activation is facilitated by increasing cellular proliferation (at least in part) probably via TNFRII and increased communication mediated by increased Cx43 protein. The identity of an additional Cx43 positive band observed at 51 kDa in response to TNF-α treatment needs further investigation. In conclusion, AGEs–RAGE interaction in human microglial CHME-5 cells results in microglial activation and excessive release of TNF-α. TNFRII and Cx43 may contribute to propagating the AGEs-mediated activation of CHME-5 cells.

7. Competing interests

Authors have no competing interests.

8. Authors' contributions

Shaikh BS developed the idea, designed and carried out the experimental work (including preparing anti-RAGE Fabs), analysed and interpreted results and prepared the manuscript. Uy B carried out AGEs characterisation, TNF-α ELISA assays and some of the western blots. Parera A carried out immunocytochemistry to check microglial activation. Nicholson LFB reviewed the manuscript. All authors read and approved the final version of the manuscript.

Acknowledgements

This work was supported by the funds from the Maurice and Phyllis Paykel Trust (Grant Nos.: 9135/3622038 and 3625865), the Faculty's Research Development Fund (University of Auckland, Grant number: 9835/3623135) and the School of Medical Foundation grant (University of Auckland, Grant number: 3625194). We thank Professor Pierre Talbot, Laboratory of Neuroimmunovirology, INRS-Institute, Armand-Frappier, Canada) for the generous gift of human microglial cell line (CHME-5) and Mrs Sailakshmi Velamoor for performing protein assays.

References

Altevogt, B.M., Paul, D.L., 2004. Four classes of intercellular channels between glial cells in the CNS. J. Neurosci. 24, 4313–4323.
Atanassov, C.L., Muller, C.D., Dumont, S., et al., 1995. Effect of ammonia on endocytosis and cytokine production by immortalized human microglia and astroglia cells. Neurochem. Int. 27, 417–424.
Becker, D.L., Green, C.R., 2002. Gap–junction mediated interactions between cells. In: Cell-Cell Interactions (T.P, F., ed): Oxford University Press, pp 47–70.
Bigl, K., Gaunitz, F., Schmitt, A., et al., 2008. Cytotoxicity of advanced glycation endproducts in human micro- and astroglial cell lines depends on the degree of protein glycation. J. Neural Transm.: Gen. Sect. 115, 1545–1556.
Brosnan, C.F., Scemes, E., Spray, D.C., 2001. Cytokine regulation of gap–junction connectivity: an open-and-shut case or changing partners at the Nexus? Am. J. Pathol. 158, 1565–1569.
Colton, C., Wilt, S., Gilbert, D., et al., 1996. Species differences in the generation of reactive oxygen species by microglia. Mol. Chem. Neuropathol. 28, 15–20.
Dalfo, E., Ferrer, I., 2005. Alpha-synuclein binding to rab3a in multiple system atrophy. Neurosci. Lett. 380, 170–175.
Dalfo, E., Portero-Otin, M., Ayala, V., et al., 2005. Evidence of oxidative stress in the neocortex in incidental Lewy body disease. J. Neuropathol. Exp. Neurol. 64, 816–830.
de Gannes, F.M.-P., Merle, M., Canioni, P., et al., 1998. Metabolic and cellular characterization of immortalized human microglial cells under heat stress. Neurochem. Int. 33, 61–73.
Dermietzel, R., Gao, Y., Scemes, E., et al., 2000. Connexin43 null mice reveal that astrocytes express multiple connexins. Brain Res. Brain Res. Rev. 32, 45–56.
Dopp, J.M., Sarafian, T.A., Spinella, F.M., et al., 2002. Expression of the p75 TNF receptor is linked to TNF-induced NFkappaB translocation and oxyradical neutralization in glial cells. Neurochem. Res. 27, 1535–1542.
Dragunow, M., 2008. The adult human brain in preclinical drug development. Nat. Rev. Drug Discovery 7, 659–666.
Dukic-Stefanovic, S., Gasic-Milenkovic, J., Deuther-Conrad, W., et al., 2003. Signal transduction pathways in mouse microglia N-11 cells activated by advanced glycation endproducts (AGEs). J. Neurochem. 87, 44–55.
Eskes, C., Juillerat-Jeanneret, L., Leuba, G., et al., 2003. Involvement of microglia–neuron interactions in the tumor necrosis factor-alpha release, microglial activation, and neurodegeneration induced by trimethyltin. J. Neurosci. Res. 71, 583–590.
Eugenin, E.A., Branes, M.C., Berman, J.W., et al., 2003. TNF-{alpha} plus IFN-{gamma} induce connexin43 expression and formation of gap–junctions between human monocytes/macrophages that enhance physiological responses. J. Immunol. 170, 1320–1328.
Eugenin, E.A., Eckardt, D., Theis, M., et al., 2001. Microglia at brain stab wounds express connexin 43 and *in vitro* form functional gap–junctions after treatment with interferon- and tumor necrosis factor-alpha. Proc. Natl. Acad. Sci. U. S. A. 98, 4190–4195.
Eugenin, E.A., Gonzalez, H.E., Sanchez, H.A., et al., 2007. Inflammatory conditions induce gap junctional communication between rat Kupffer cells both *in vivo* and *in vitro*. Cell. Immunol. 247, 103–110.
Fonseca, C.G., Green, C.R., Nicholson, L.F., 2002. Upregulation in astrocytic connexin 43 gap–junction levels may exacerbate generalized seizures in mesial temporal lobe epilepsy. Brain Res. 929, 105–116.
Gao, H.-M., Jiang, J., Wilson, B., et al., 2002. Microglial activation-mediated delayed and progressive degeneration of rat nigral dopaminergic neurons: relevance to Parkinson's disease. J. Neurochem. 81, 1285–1297.
Garg, S., Md Syed, M., Kielian, T., 2005. Staphylococcus aureus-derived peptidoglycan induces Cx43 expression and functional gap–junction intercellular communication in microglia. J. Neurochem. 95, 475–483.
Gefter, J.V., Shaufl, A.L., Fink, M.P., et al., 2009. Comparison of distinct protein isoforms of the receptor for advanced glycation end-products expressed in murine tissues and cell lines. Cell Tissue Res. 337, 79–89.
Graeber, M.B., Bise, K., Mehraein, P., 1994. CR3/43, a marker for activated human microglia: application to diagnostic neuropathology. Neuropathol. Appl. Neurobiol. 20, 406–408.
He, J., Crews, F.T., 2008. Increased MCP-1 and microglia in various regions of the human alcoholic brain. Exp. Neurol. 210, 349–358.
Horikoshi, Y., Sasaki, A., et al., 2003. Human GLUT5 immunolabeling is useful for evaluating microglial status in neuropathological study using paraffin sections. Acta Neuropathol. 105, 157–162.
Janabi, N., Peudenier, S., Heron, B., et al., 1995. Establishment of human microglial cell lines after transfection of primary cultures of embryonic microglial cells with the SV40 large T antigen. Neurosci. Lett. 195, 105–108.
Kawanokuchi, J., Mizuno, T., Takeuchi, H., et al., 2006. Production of interferon-gamma by microglia. Mult. scler. (Houndmills, Basingstoke, England) 12, 558–564.
Kielian, T., 2008. Glial connexins and gap–junctions in CNS inflammation and disease. J. Neurochem. 106, 1000–1016.

Kuhla, B., Loske, C., Garcia De Arriba, S., 2004. Differential effects of "Advanced glycation endproducts" and beta-amyloid peptide on glucose utilization and ATP levels in the neuronal cell line SH-SY5Y. J. Neural Transm.: Gen. Sect. 111, 427–439.

Lawson, L.J., Perry, V.H., Dri, P., et al., 1990. Heterogeneity in the heterogeneity in the distribution and morphology of microglia in the normal adult mouse brain. Neurosci. Lett. 39, 151–170.

Lue, L.F., Walker, D.G., Brachova, L., et al., 2001. Involvement of microglial receptor for advanced glycation endproducts (RAGE) in Alzheimer's disease: identification of a cellular activation mechanism. Exp. Neurol. 171, 29–45.

Lue, L.F., Yan, S.D., Stern, D.M., et al., 2005. Preventing activation of receptor for advanced glycation endproducts in Alzheimer's disease. Curr. Drug Targets CNS Neurol. Disord. 4, 249–266.

Macouillard-Poulletier de Gannes, F., Leducq, N., Diolez, P., et al., 2000. Mitochondrial impairment and recovery after heat shock treatment in a human microglial cell line. Neurochem. Int. 36, 233–241.

McGeer, E.G., McGeer, P.L., 1997. The role of the immune system in neurodegenerative disorders. Mov. Disord. 12, 855–858.

McGeer, P.L., Itagaki, S., Boyes, B.E., et al., 1988. Reactive microglia are positive for HLA-DR in the substantia nigra of Parkinson's and Alzheimer's disease brains. Neurology 38, 1285–1291.

Munch, G., Gasic-Milenkovic, J., Dukic-Stefanovic, S., et al., 2003. Microglial activation induces cell death, inhibits neurite outgrowth and causes neurite retraction of differentiated neuroblastoma cells. Exp. Brain Res. 150, 1–8.

Munch, G., Gerlach, M., Sian, J., et al., 1998. Advanced glycation end products in neurodegeneration: more than early markers of oxidative stress? Ann. Neurol. 44, S85–88.

Munch, G., Luth, H.J., Wong, A., et al., 2000. Crosslinking of alpha-synuclein by advanced glycation endproducts–an early pathophysiological step in Lewy body formation? J. Chem. Neuroanat. 20, 253–257.

Nagai, A., Nakagawa, E., Hatori, K., et al., 2001. Generation and characterization of immortalized human microglial cell lines: expression of cytokines and chemokines. Neurobiol. Dis. 8, 1057–1068.

Nagatsu, T., Sawada, M., 2007. Biochemistry of postmortem brains in Parkinson's disease: historical overview and future prospects. J. Neural Transm.: Gen. Sect. (Suppl.), 113–120.

Neumann, A., Schinzel, R., Palm, D., et al., 1999. High molecular weight hyaluronic acid inhibits advanced glycation endproduct-induced NF-[kappa]B activation and cytokine expression. FEBS Lett. 453, 283–287.

O'Carroll, S.J., Alkadhi, M., Nicholson, L.F., et al., 2008. Connexin 43 mimetic peptides reduce swelling, astrogliosis, and neuronal cell death after spinal cord injury. Cell Commun. Adhes. 15, 27–42.

Osawa, M., Yamamoto, Y., Munesue, S., et al., 2007. De-N-glycosylation or G82S mutation of RAGE sensitizes its interaction with advanced glycation endproducts. Biochim. Biophys. Acta 1770, 1468–1474.

Pahujaa, M., Anikin, M., Goldberg, G.S., 2007. Phosphorylation of connexin43 induced by Src: regulation of gap junctional communication between transformed cells. Exp. Cell Res. 313, 4083–4090.

Park, S.J., Kleffmann, T., Hessian, P.A., 2011. The G82S polymorphism promotes glycosylation of the receptor for advanced glycation end products (RAGE) at Asn81: a comparison of wild-type RAGE with the G82S polymorphic variant. J. Biol. Chem.

Peppa, M., Uribarri, J., Vlassara, H., 2003. Glucose, advanced glycation end products, and diabetes complications: what is new and what works. Clin. Diabetes 21, 186–187.

Peudenier, S., Hery, C., Montagnier, L., et al., 1991. Human microglial cells: characterization in cerebral tissue and in primary culture, and study of their susceptibility to HIV-1 infection. Ann. Neurol. 29, 152–161.

Ramasamy, R., Vannucci, S.J., Yan, S.S., et al., 2005. Advanced glycation end products and RAGE: a common thread in aging, diabetes, neurodegeneration, and inflammation. Glycobiology 15, 16R–28R.

Rash, J.E., Yasumura, T., Davidson, K.G., et al., 2001. Identification of cells expressing Cx43, Cx30, Cx26, Cx32 and Cx36 in gap–junctions of rat brain and spinal cord. Cell Commun. Adhes. 8, 315–320.

Rogers, J., Luber-Narod, J., Styren, S.D., et al., 1988. Expression of immune system-associated antigens by cells of the human central nervous system: relationship to the pathology of Alzheimer's disease. Neurobiol. Aging 9, 339–349.

Saez, J.C., Martinez, A.D., Branes, M.C., et al., 1998. Regulation of gap–junctions by protein phosphorylation. Braz. J. Med. Biol. Res. 31, 593–600.

Sasaki, A., Yamaguchi, H., Horikoshi, Y., et al., 2004. Expression of glucose transporter 5 by microglia in human gliomas. Neuropathol. Appl. Neurobiol. 30, 447–455.

Sasaki, A., Yamaguchi, H., Ogawa, A., et al., 1997. Microglial activation in early stages of amyloid β protein deposition. Acta Neuropathol. 94, 316–322.

Schmidt, A.M., Yan, S.D., Yan, S.F., et al., 2000. The biology of the receptor for advanced glycation end products and its ligands. Biochim. Biophys. Acta 1498, 99–111.

Schmitt, A., Bigl, K., Meiners, I., et al., 2006. Induction of reactive oxygen species and cell survival in the presence of advanced glycation end products and similar structures. Biochim. Biophys. Acta, Mol. Cell Res. 1763, 927–936.

Schmitt, A., Meiners, I., Schmitt, J., et al., 2005a. Two analytical methods to study the interaction of AGEs with cell surface proteins. J. Biochem. Biophys. Methods 65, 121–136.

Schmitt, A., Schmitt, J., Munch, G., et al., 2005b. Characterization of advanced glycation end products for biochemical studies: side chain modifications and fluorescence characteristics. Anal. Biochem. 338, 201–215.

Shaikh, S., Nicholson, L.F., 2006. Optimization of the Tet-On system for inducible expression of RAGE. J. Biomol. Tech. 17, 283–292.

Shaikh, S., Nicholson, L.F., 2008. AGEs induce *in vitro* cross-linking of alpha-synuclein and accelerate the process of intracellular inclusion body formation. J. Neurosci. Res. 86, 2071–2082.

Shaikh, S.B., Nicholson, L.F., 2009. Effects of chronic low dose rotenone treatment on human microglial cells. Mol. Neurodegener. 4, 55.

Shavali, S., Combs, C., Ebadi, M., 2006. Reactive macrophages increase oxidative stress and alpha-synuclein nitration during death of dopaminergic neuronal cells in co-culture: relevance to Parkinson's disease. Neurochem. Res. 31, 85–94.

Sherer, T.B., Betarbet, R., Kim, J.H., et al., 2003. Selective microglial activation in the rat rotenone model of Parkinson's disease. Neurosci. Lett. 341, 87–90.

Solan, J., Lampe, P., 2007. Key connexin 43 phosphorylation events regulate the gap–junction life cycle. J. Membr. Biol. 217, 35–41.

Takeuchi, H., Jin, S., Wang, J., et al., 2006. Tumor necrosis factor-alpha induces neurotoxicity via glutamate release from hemichannels of activated microglia in an autocrine manner. J. Biol. Chem. 281, 21362–21368.

Thery, C., Mallat, M., 1993. Influence of interleukin-1 and tumor necrosis factor alpha on the growth of microglial cells in primary cultures of mouse cerebral cortex: involvement of colony-stimulating factor 1. Neurosci. Lett. 150, 195–199.

Valencia, J.V., Weldon, S.C., Quinn, D., et al., 2004. Advanced glycation end product ligands for the receptor for advanced glycation end products: biochemical characterization and formation kinetics. Anal. Biochem. 324, 68–78.

Vandamme, W., Braet, K., Cabooter, L., et al., 2004. Tumour necrosis factor alpha inhibits purinergic calcium signalling in blood-brain barrier endothelial cells. J. Neurochem. 88, 411–421.

Wang, A.L., Yu, A.C., He, Q.H., et al., 2007. AGEs mediated expression and secretion of TNF alpha in rat retinal microglia. Exp. Eye Res. 84, 905–913.

Wang, C.Y., Liu, H.J., Chen, H.J., et al., 2011. AGE-BSA down-regulates endothelial connexin43 gap–junctions. BMC Cell Biol. 12, 19.

Wong, A., Luth, H.J., Deuther-Conrad, W., et al., 2001. Advanced glycation endproducts co-localize with inducible nitric oxide synthase in Alzheimer's disease. Brain Res. 920, 32–40.

Yan, S.D., Chen, X., Fu, J., et al., 1996. RAGE and amyloid-beta peptide neurotoxicity in Alzheimer's disease. Nature 382, 685–691.

Yan, S.D., Stern, D., Kane, M.D., et al., 1998. RAGE-Abeta interactions in the pathophysiology of Alzheimer's disease. Restor. Neurol. Neurosci. 12, 167–173.

Yan, S.F., Ramasamy, R., Naka, Y., et al., 2003. Glycation, inflammation, and RAGE: a scaffold for the macrovascular complications of diabetes and beyond. Circ. Res. 93, 1159–1169.